applied sciences

MDPI

Article

Thorium Recovery with Crown Ether–Polymer Composite Membranes

Aurelia Cristina Nechifor [1], Paul Constantin Albu [2], Ludmila Motelica [3], Geani Teodor Man [1,4], Alexandra Raluca Grosu [1], Szidonia-Katalin Tanczos [5], Vlad-Alexandru Grosu [6,*], Virgil Emanuel Marinescu [7] and Gheorghe Nechifor [1,*]

1 Analytical Chemistry and Environmental Engineering Department, National University of Science and Technology Politehnica Bucharest, 011061 Bucharest, Romania; aureliacristinanechifor@gmail.com (A.C.N.); andra.grosu@upb.ro (A.R.G.); geani.man@icsi.ro (G.T.M.)
2 Radioisotopes and Radiation Metrology Department (DRMR), IFIN Horia Hulubei, 023465 Măgurele, Romania; paulalbu@gmail.com
3 National Research Center for Micro and Nanomaterials, Department of Science and Engineering of Nanomaterials and Oxide Materials, National University of Science and Technology Politehnica Bucharest, 060042 Bucharest, Romania; ludmila.motelica@upb.ro
4 National Research and Development Institute for Cryogenics and Isotopic Technologies–ICSI, 240050 Râmnicu-Vâlcea, Romania
5 Department of Bioengineering, University Sapientia of Miercurea-Ciuc, 500104 Miercurea-Ciuc, Romania; tczszidonia@yahoo.com
6 Department of Electronic Technology and Reliability, Faculty of Electronics, Telecommunications and Information Technology, National University of Science and Technology Politehnica Bucharest, 061071 Bucharest, Romania
7 Department of Physical-Chemical Tests, National Institute for Research and Development in Electrical Engineering ICPE–CA Bucharest, 030138 Bucharest, Romania; virgil.marinescu@icpe-ca.ro
* Correspondence: vlad.grosu@upb.ro (V.-A.G.); gheorghe.nechifor@upb.ro (G.N.)

Abstract: Thorium is a weak radioactive element, but the control of its concentration in natural aqueous systems is of great interest for health, because it is a toxic heavy metal. The present paper presents the recovery of thorium from diluted synthetic aqueous systems by nanofiltration. The membranes used for the nanofiltration of systems containing thorium species are composites containing 4′-Aminobenzo-15-crown-5 ether (ABCE) and sulfonated poly–etherether–ketone (sPEEK). The composite membranes (ABCE–sPEEK) were characterized by scanning electron microscopy (SEM), energy-dispersive X–Ray spectroscopy (EDAX), thermal analysis (TG and DSC), and from the perspective of thorium removal performance. To determine the process performance, the variables were the following: the nature of the composite membrane, the concentration of thorium in the aqueous systems, the rotation speed of the stirrer, and the pressure and the pH of the thorium aqueous system. When using pure water, a permeate flux value of 12 $L \cdot m^{-2}$ h^{-1} was obtained for the sPEEK membrane, and a permeate flux value of up to 15 $L \cdot m^{-2}$ h^{-1} was obtained for the ABCE–sPEEK composite membrane. The use of mechanical stirring, with a propeller stirrer, lead to an increase in the permeate flux value of pure water by about 20% for each of the studied membranes. Depending on the concentration of thorium and the pH of the feed solution, retentions between 84.9% and 98.4% were obtained. An important observation was the retention jump at pH 2 for the ABCE–sPEEK composite membrane. In the paper, a thorium ion retention mechanism is proposed for the sPEEK membrane and the ABCE–sPEEK composite membrane.

Keywords: thorium; thorium removing; thorium recovery; composite membranes; crown ether; sulfonated poly–ether–ether–ketone (sPEEK)

check for updates

Citation: Nechifor, A.C.; Albu, P.C.; Motelica, L.; Man, G.T.; Grosu, A.R.; Tanczos, S.-K.; Grosu, V.-A.; Marinescu, V.E.; Nechifor, G. Thorium Recovery with Crown Ether–Polymer Composite Membranes. *Appl. Sci.* **2024**, *14*, 9937. https://doi.org/10.3390/app14219937

Academic Editors: Alexandra Bargan and Alina Soroceanu

Received: 26 September 2024
Revised: 20 October 2024
Accepted: 28 October 2024
Published: 30 October 2024

Copyright: © 2024 by the authors. Licensee MDPI, Basel, Switzerland. This article is an open access article distributed under the terms and conditions of the Creative Commons Attribution (CC BY) license (https://creativecommons.org/licenses/by/4.0/).

1. Introduction

Thorium is a weak radioactive element, with an abundance similar to that of lead [1–3]. From this point of view, thorium should not concern environmental protection researchers [4].

However, what must be considered is that thorium is a heavy metal, with a potential toxicity similar to other heavy metals [5,6]. A special feature of thorium is its presence in various surface waters [6,7], soil [8], and it can even accumulate in various plants [8]. It is expected that thorium appears in mining areas in aqueous effluents [9], but also naturally in streams or rivers that pass-through areas where thorium is accumulated [9,10]. At a common pH of surface waters [11], thorium precipitates and is found in sediments, but under acidic water conditions thorium is found in the ionic form Th^{4+}, or the hydroxyl forms $Th(OH)^{3+}$, $Th(OH)_2^{2+}$, $Th(OH)_3^{+}$ [12,13].

Thus, the recovery of thorium from aqueous systems containing thorium or other heavy metals becomes extremely important [14]. Classical separation processes (precipitation, sedimentation, flocculation, ion exchange) can be taken into account [15,16], but modern extractive, adsorptive, and membrane processes can also be approached (Table 1) [17–33].

Table 1. The main techniques and methods of thorium recovery.

Techniques or Methods of Thorium Recovery	Refs.
Polymer inclusion membrane	[17]
Ionic liquid Cyphos IL 104.	[18]
α–Aminophosphonates, –phosphinates, and –phosphine oxides as extraction and precipitation agents	[19]
Polymeric materials	[20]
Highly efficient adsorbent	[21]
Binary extractant based on 1,5–bis [2–(hydroxyethoxyphosphoryl) –4–ethylphenoxy] –3–oxapentane and methyl trioctylammonium nitrate	[22]
2–nitroso–1–naphthol impregnated MCI GEL CHP20P resin	[23]
UiO–66–OH zirconium metal–organic framework	[24]
Polyurea-crosslinked alginate aerogels	[25]
α–Aminophosphonate extractant	[26]
8–Hydroxyquinoline-immobilized bentonite	[27]
New polymer with imprinted ions	[28]
Zeolite adsorption	[29]
Nanofiltration membrane	[30]
Ionic liquids	[31,32]
Nanofiltration extraction	[33]

From a practical point of view, to obtain thorium-free drinking water, the use of emulsion membranes is excluded due to the need for reagents and solvents which would impurify the water and, at the same time, attempting recovery by breaking the emulsions raises problems difficult to solve in the isolated areas that we have in view [34,35]. If an approach based on a membrane technique is desired, then one that uses hollow fiber membranes is viable [36,37]. The beginning of an application with hollow fiber membranes occurs, most of the time and in the present study, with the study of separation with bulk or flat membranes [38–40].

An accessible and efficient procedure is nanofiltration, which uses nanoporous composite membranes and achievable pressures (4–8 atm) with usual means [41–45].

The proposed thorium separation process is expected to perform with a similar, complementary, or superior performance to those previously presented [17–33], according to Table 2.

Table 2. The performance expected for thorium separation of the proposed process compared to other processes.

Processes	Methods or Processes Characteristics						
	Selectivity/ Retention	Flux	Residues	Operation in Isolated Locations	Reagents or Auxiliary Materials	Scale-Up	Investments
Proposed process	***	***	***	***	***	***	***
Ionic liquids	***	**	*	*	*	*	*
Polymer inclusion membrane	***	*	***	*	**	*	**
Adsorption	***	***	**	**	**	***	***
Imprinted polymer	***	*	***	**	***	***	***
Extraction	***	***	*	*	*	***	*

(***) very favorable; (**) favorable; (*) less favorable.

In the present work, the separation of thorium in ionic form, from dilute aqueous solutions similar to those found in isolated places, is addressed, so as to obtain drinking water.

The issue that we propose as a study is the separation of thorium from synthetic solutions using the dead-end filtration technique, with sulfonated poly-ether-ether-sulfonate ketone (sPEEK) membranes containing 4′–Amino–Benzo15–Crown5 Ether (ABCE).

Compared to the results previously presented for the separation of thorium with sPEEK membranes [45], in this work it is proposed to use an ionic–ionic-complexing composite membrane, which allows efficient separation of the flux and retention of the Th^{4+} ion from acidic media.

2. Materials and Methods

2.1. Reagents and Materials

All reagents and organic compounds used in the presented work were of analytical grade.

Th $(NO_3)_4 \cdot 5H_2O$, HNO_3 (65%), H_2SO_4 (96%), NaOH pellets, HCl 35% super pure, and NH_4OH 25% (analytical grade) were purchased from Merck KGaA (Darmstadt, Germany).

Thorin, $C_{16}H_{11}AsN_2Na_2O_{10}S_2$, 1-(2-Arsonophenylazo)-2-hydroxy-3,6-naphthalene-disulfonic acid sodium salt, or 2-(2-Hydroxy-3,6-disulfo-1-naphthylazo)-benzene-arsonic acid sodium salt; (Benzo-15-crown-5)-4′-ylamine, or 4′–Amino–Benzo15–Crown–5 Ether (ABCE); and Poly(oxy-1,4-phenyleneoxy-1,4-phenylenecarbonyl-1,4-phenylene), or Poly Ether Ether Ketone (PEEK) purchased from Sigma-Aldrich Chemie GmbH (Steinheim, Germany) were used within the study.

The purified water characterized by 18.2 μS/cm conductivity was obtained with an RO Millipore system (MilliQ® Direct 8 RO Water Purification System, Merck KGaA (Darmstadt, Germany) [16].

2.2. Procedures and Methods

2.2.1. Preparation of the sPEEK Membranes

The preparation of sPEEK membranes using a solution of PEEK in 96% sulfuric acid was previously reported (Figure 1) [45,46]. In short, the predetermined amount of PEEK is dissolved in 96% sulfuric acid by stirring in an ultrasonic bath, for 48 h. After dissolution, a solution is obtained in which PEEK has transformed into sPEEK through a chemical reaction at ambient temperature. The sPEEK gel is deposited on a Petri glass support. The film formed on the Petri dish is placed in a vacuum oven, with laminar air flow, at a temperature of 50 °C, for 72 h. After the drying interval, the sPEEK membrane is cut to the size required for the nanofiltration experiments.

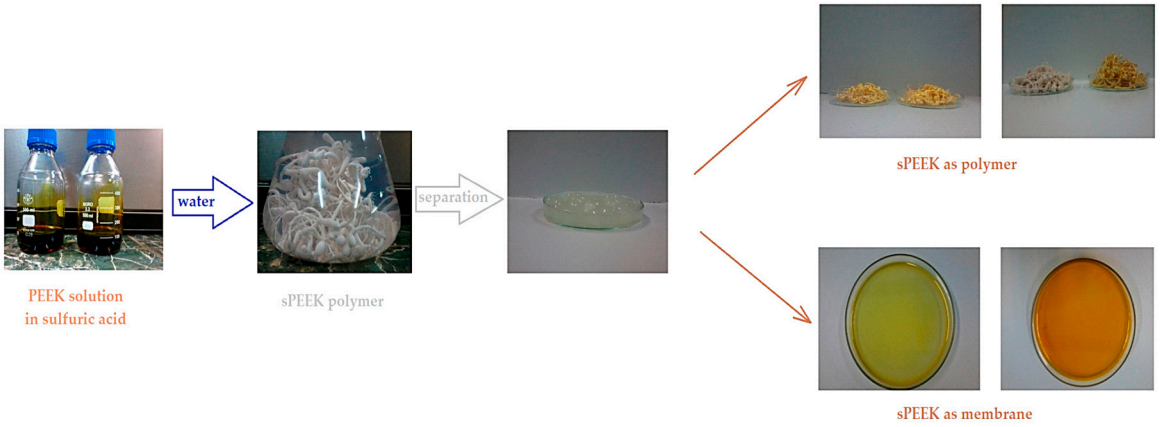


Figure 1. Preparation of sPEEK membranes from PEEK solution in sulfuric acid [46].

sPEEK membranes were characterized by scanning electron microscopy (SEM), energy-dispersive X–Ray spectroscopy (EDAX), and thermal analysis (TG and DSC).

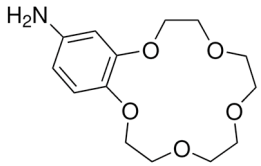
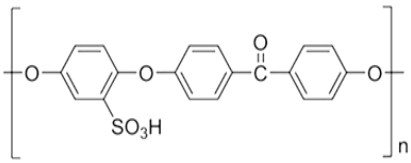
The determination of the degree of sulfonation and the ion capacity exchange (i.c.e. = 1.65 mmol/g) were reported [47–49].

2.2.2. Preparation of ABCE–sPEEK Composite Membranes

4′–Amino–Benzo–15–Crown–5 Ether–sPEEK composite membranes (ABCE–sPEEK) were obtained by dissolving the crown ether (ABCE) in a concentration of 1.65 mmol/g sPEEK, in the sPEEK solution whose preparation was previously described, after which the steps specified and illustrated in Figure 1 were followed.

The characteristics of the composite membrane compounds are shown in Table 3.

Table 3. The characteristics of the components of the composite membrane preparation.

Organic Compounds	Name and Symbol	Solubility	pKa
	4′–Amino–Benzo–15–Crown–5 Ether (ABCE)	organic polar solvents	4.63
	sulfonated Poly Ether–Ether–Ketone (sPEEK)	organic polar solvents	2.0 to 2.2

Composite membranes (ABCE–sPEEK) were characterized by scanning electron microscopy (SEM), energy-dispersive X-Ray spectroscopy (EDAX), and thermal analysis (TG and DSC).

2.2.3. Nanofiltration Experiments

Nanofiltration of the thorium nitrate solution was carried out (Figure 2) at a pressure of 5 to 9 atmospheres through the composite membrane (ABCE–sPEEK) and for comparison through the sPEEK membrane. The module of nanofiltration, of a dead-end filtration type, is equipped with a propeller stirrer that performs a turbulent agitation of the feed solution. The feed solutions have a concentration of 10^{-4} mol/L and 10^{-5} mol/L thorium nitrate in ultrapure water also containing nitric acid. The pH variation of these solutions is conducted with nitric acid solutions of 1 mol/L, 10^{-1} mol/L, 10^{-2} mol/L, 10^{-3} mol/L, and 10^{-4} mol/L. The surface of the membrane in the nanofiltration module is 100 ± 0.3 cm^2.

The capacity of the module is 2000 cm^3. The propeller stirrer has a diameter of 7 cm and can be rotated from 50 rpm to 250 rpm.

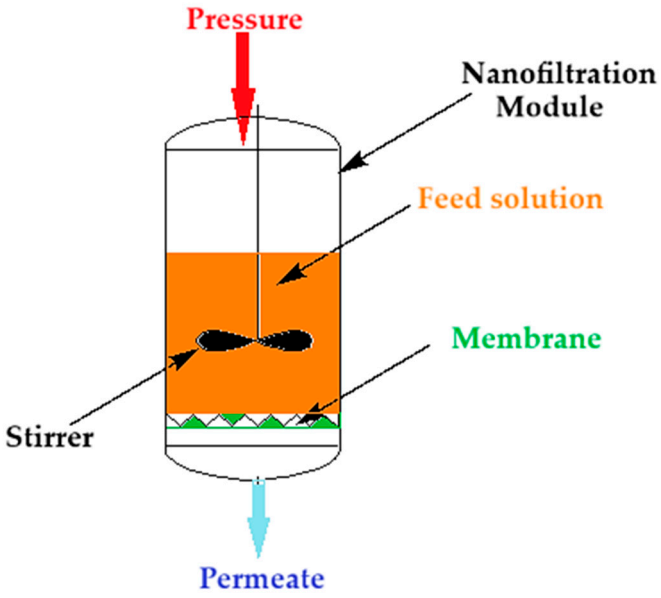


Figure 2. Schematic presentation of the nanofiltration module of the thorium solution.

The result of the nanofiltration was presented in the form of the permeate flux (J) (Equation (1)) or of the nanofiltration retention [50] (R) (Equation (2)):

$$J = \frac{V}{S \cdot \Delta t}\left(L/m^2h\right) \quad (1)$$

where: J—permeate flux; V—permeate volume; S—surface of the membrane; Δt—operating interval;

$$R(\%) = \frac{(C_0 - C_f)}{C_0} \times 100 \quad (2)$$

where: R—retention (%); C_0—concentration of feed solution; C_f—final concentration.

The concentration of the thorium ion was determined by the Thorin spectrophotometric method. The specific determinations are carried out through coupled extraction separation and spectrophotometric detection at λ = 495 nm. The detection limit of the method is 0.04 μg Th (IV) mL^{-1}, and the RSD (n = 10) is 1.4% [51]. The obtained results have a total precision of 0.1 ppm imposed both by the traceability of the samples taken and by the spectrophotometric methods approached.

When establishing the accuracy of 0.1 ppm, the following factors were taken into account: the measurement deviation of the sample volume taken from nanofiltration, the pH adjustment deviation of the permeate solution, the deviation from the selected wavelength compared to that of the absorption maximum, the temperature variation during the determinations, the validation on two different spectrometric devices, the independent work of two analysts, and the reduced number of repeated determinations (five).

2.3. Equipment

For the study of the scanning electron microscopy (SEM) and energy-dispersive spectrum for the characteristic X-Ray (EDAX) analyses, the membrane samples, subjected to the analysis, were visualized with the help of the FESEM–FIB workstation (scanning electron microscope with field emission electron and focused beam of ions), model Auriga (Carl Zeiss SMT, Oberkochen, Germany), by means of the secondary electron/ion detector (SESI) in the sample chamber for the topography/morphology of the surface of the analyzed samples [52].

The verification of the chemical composition was carried out with the help of the EDS probe produced by Oxford Instruments, UK—energy-dispersive spectrometer model X-MaxN with Aztec acquisition and processing software integrated on the FESEM–FIB Auriga working station [53].

The validation of scanning microscopy studies (SEM and HR–SEM) was performed using a Hitachi S4500 system (Hitachi High-Tech Europe GmbH, Mannheim, Germany) [54–56].

Thermal analysis (TG-DSC) was performed with STA 449C Jupiter apparatus, from Netzsch (NETZSCH-Gerätebau GmbH, Selb, Germany). Each sample was weighed at approximatively 10 mg. The samples were placed in an open alumina crucible and heated up to 900 °C with a 10 K·min^{-1} rate, under a flow of 50 mL·min^{-1} dried air. As a reference, we used an empty alumina crucible [54].

The UV-Vis analyses of the solutions were performed on a Spectrometer CamSpec M550 (Spectronic CamSpec Ltd., Leeds, UK) [55].

The UV-Vis studies on the samples' composition were validated on dual-beam UV equipment—Varian Cary 50 (Agilent Technologies Inc., Santa Clara, CA, USA) at a resolution of 1 nm, a spectral bandwidth of 1.5 nm, and a 300 nm/s scan rate. The UV-Vis spectra of the samples were recorded for a wavelength from 200 to 800 nm, at room temperature, using 10 mm quartz cells [56].

The pH of the medium was followed up with a combined selective electrode (HI4107, Hanna Instruments Ltd., Leighton Buzzard, UK) and a multi-parameter system (HI5522, Hanna Instruments Ltd., Leighton Buzzard, UK) [57].

Other devices used were as follows: ultrasonic bath (Elmasonic S, Elma Schmidbauer GmbH, Singen, Germany), vacuum oven (VIOLA—Shimadzu, Bucharest, Romania) [58].

3. Results and Discussion

The morphological and structural characterizations of the prepared membranes were carried out by scanning electron microscopy (SEM), energy-dispersive X–Ray spectroscopy (EDAX), and thermal analysis (TG and DSC), and the performance in the retention process of thorium from acidic aqueous solutions was established by determining the permeate fluxes (J) and thorium retention (R%).

3.1. Characterization of the Prepared Membranes

3.1.1. Morphological Characterization

The section morphology of the two membranes—the sPEEK membrane and the ABCE–sPEEK composite membrane—was examined in the section and on the bottom surface using scanning electron microscopy (SEM) (Figures 3a–c and 4a–c). The images were obtained using the FESEM–FIB workstation on samples fractured in liquid nitrogen and without metallization.

The images in Figures 3d and 4d were obtained after the metallization of the top surfaces of the membranes with a gold layer of about 50 nm.

The section of the sPEEK membrane (Figure 3a) is a porous structure (orange arrows) in which a selective, more compact upper layer can be observed (red arrow). The bottom surface of the membrane (Figure 3b,c) has submicron pores.

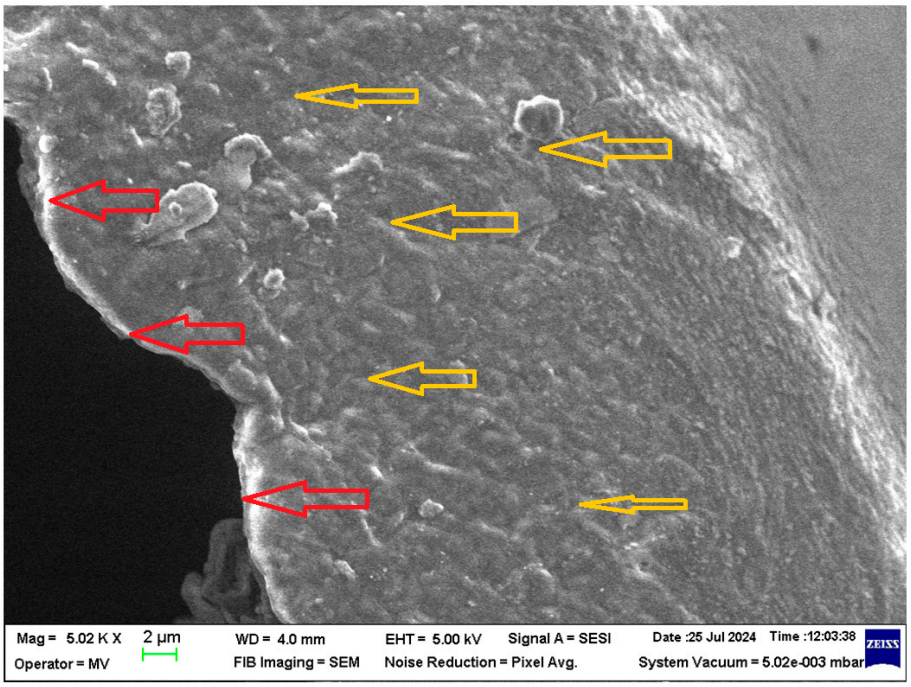
The section of the ABCE–sPEEK composite membrane is also compact at the selective layer (Figure 4a, red arrows) and porous (Figure 4a, orange arrows). The bottom layer reveals uniform micro-porosity (Figure 4b,c).

At a magnification of 40,000×, the compactness of the two membranes can be observed on the top surfaces (Figures 3d and 4d). Most likely, the pores are nanometric.

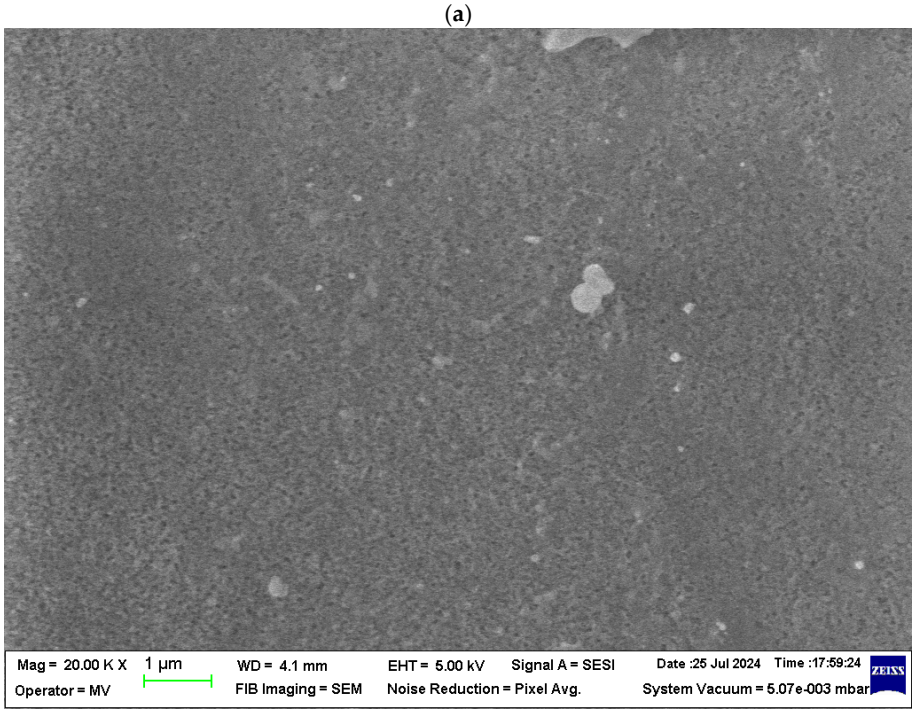
From the point of view of the membrane surfaces, the pore size on the bottom surface of the sPEEK membrane (Figure 3b,c) is smaller than that of the pores of the ABCE–sPEEK composite membranes (Figure 4b,c). On the top surfaces, the size of the nanopores of the two membranes (Figures 3d and 4d) is almost similar.

In section (Figures 3a and 4a), the difference between the two membranes is significant. The sPEEK membrane is less porous (more compact) (Figure 3a) than the ABCE–sPEEK membrane which is looser (Figure 4a).

Although they have a different structure, both in section and on the bottom surfaces, these membranes are likely to be used for the nanofiltration of solutions containing ionic thorium, because the materials from which they are made are ion exchangers and/or complexants.

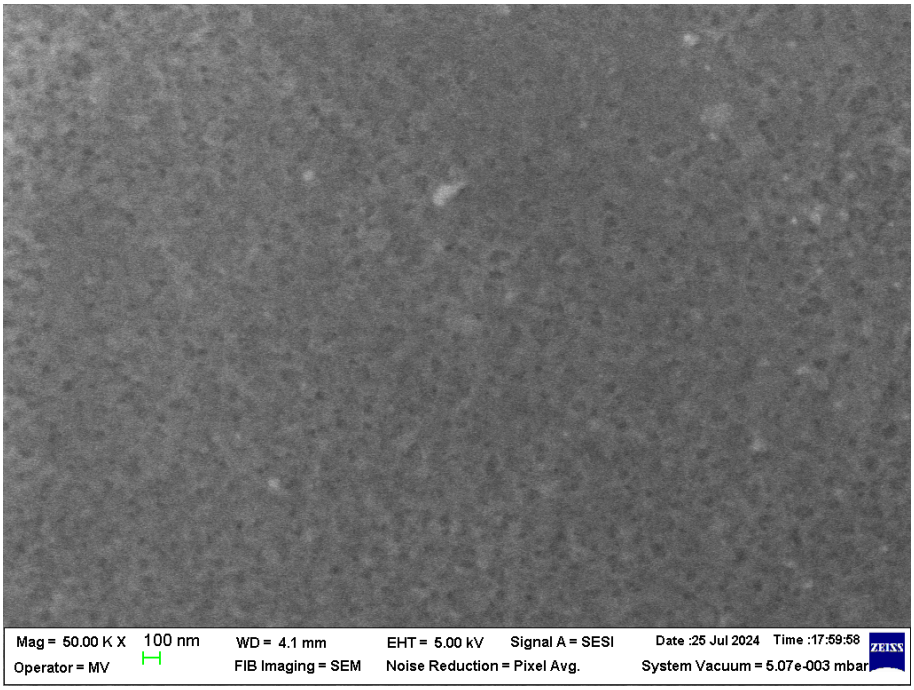


(**a**)

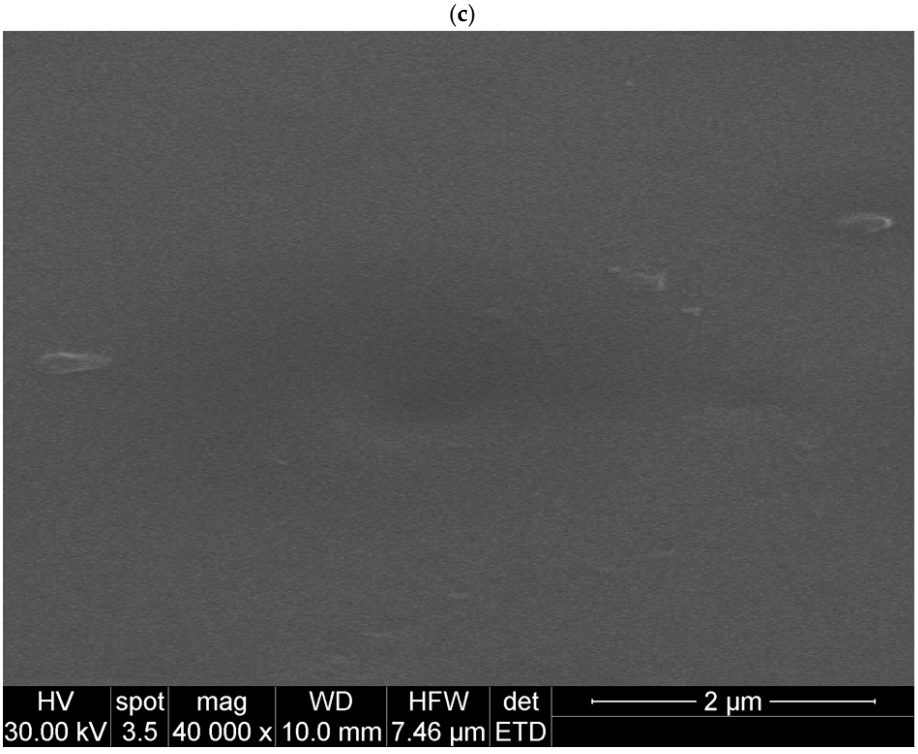


(**b**)

Figure 3. *Cont.*

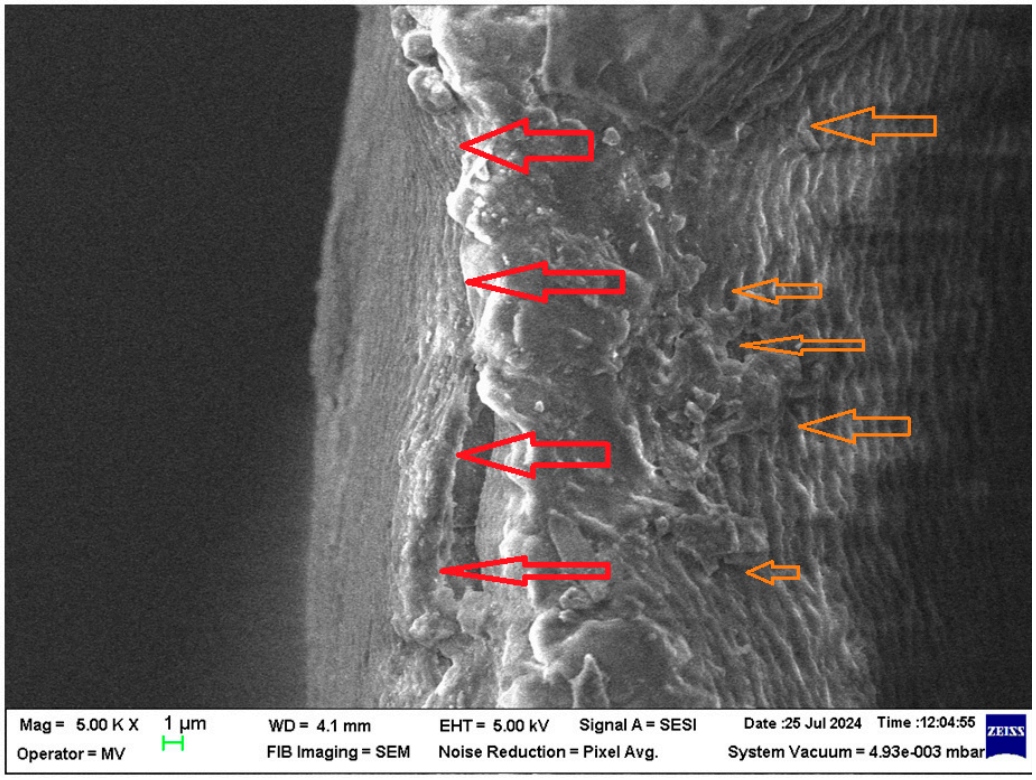


(**c**)

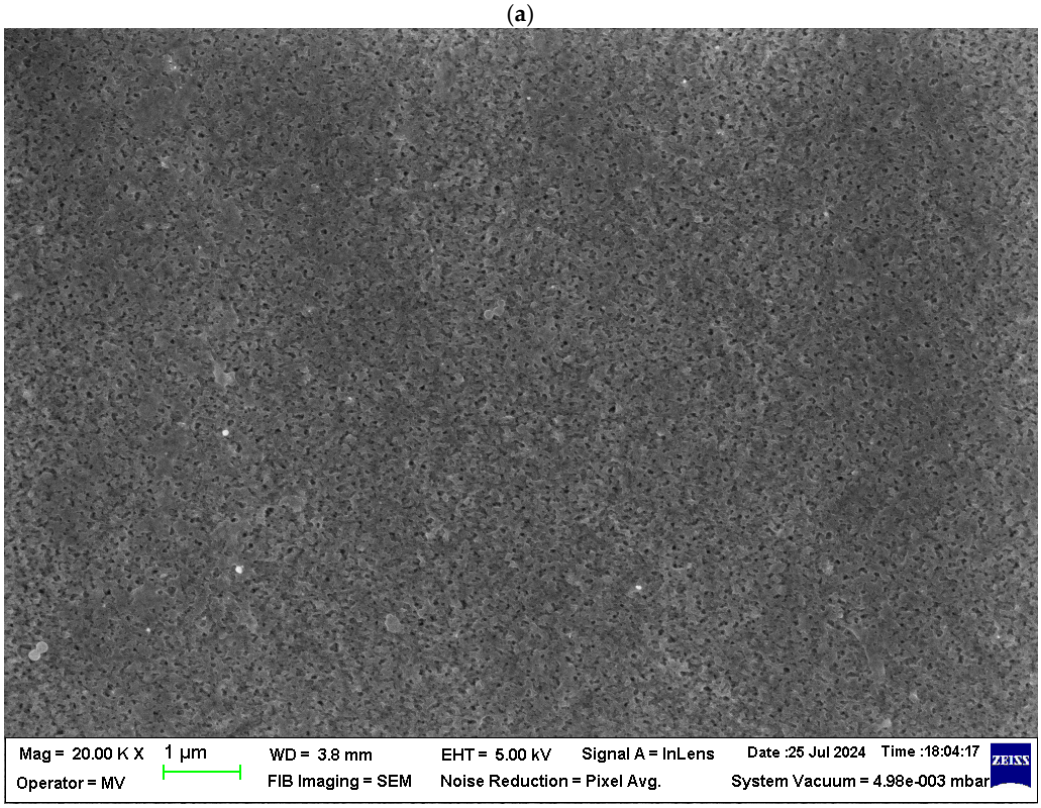


(**d**)

Figure 3. Scanning electron microscopy (SEM) images of the sPEEK membrane: (**a**) section; (**b**) bottom surface; (**c**) detail of the bottom surface (50,000×); and (**d**) detail of the top surface (40,000×).

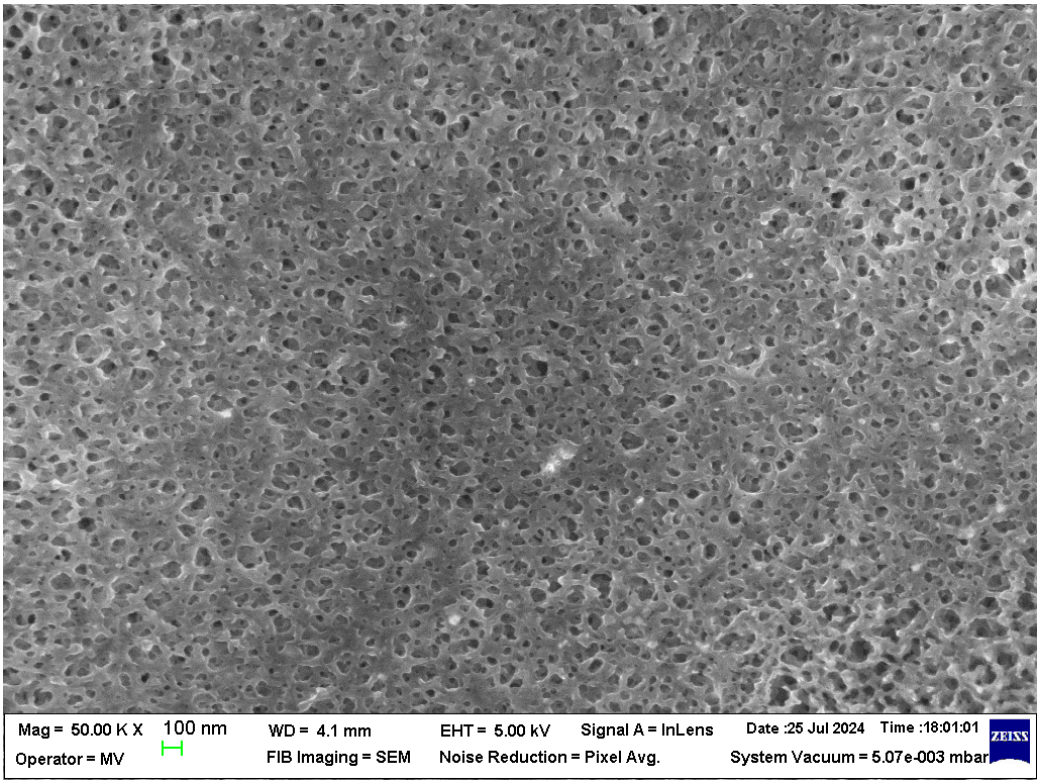


(**a**)

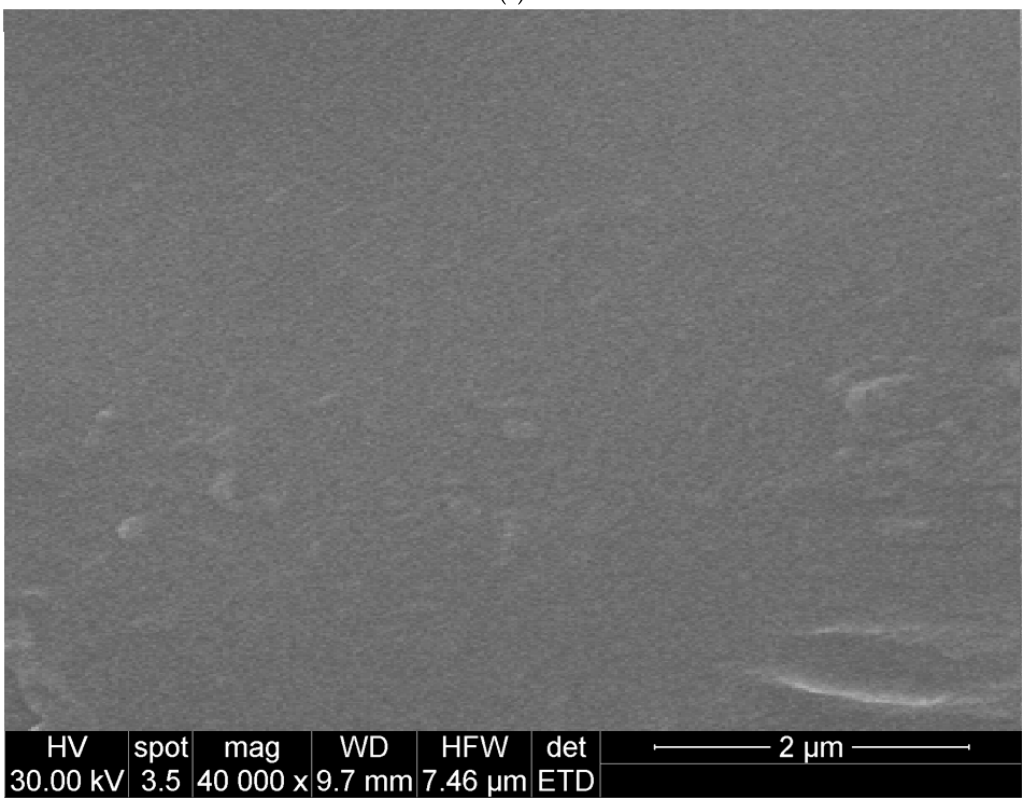


(**b**)

Figure 4. *Cont*.



(**c**)



(**d**)

Figure 4. Scanning electron microscopy (SEM) images of the ABCE–sPEEK composite membrane: (**a**) section; (**b**) bottom surface; (**c**) detail of the bottom surface (50,000×); and (**d**) detail of the top surface (40,000×).

3.1.2. Compositional Analysis

Compositional analysis (EDAX) was performed on the surface of the membranes (Figure 5a,b).

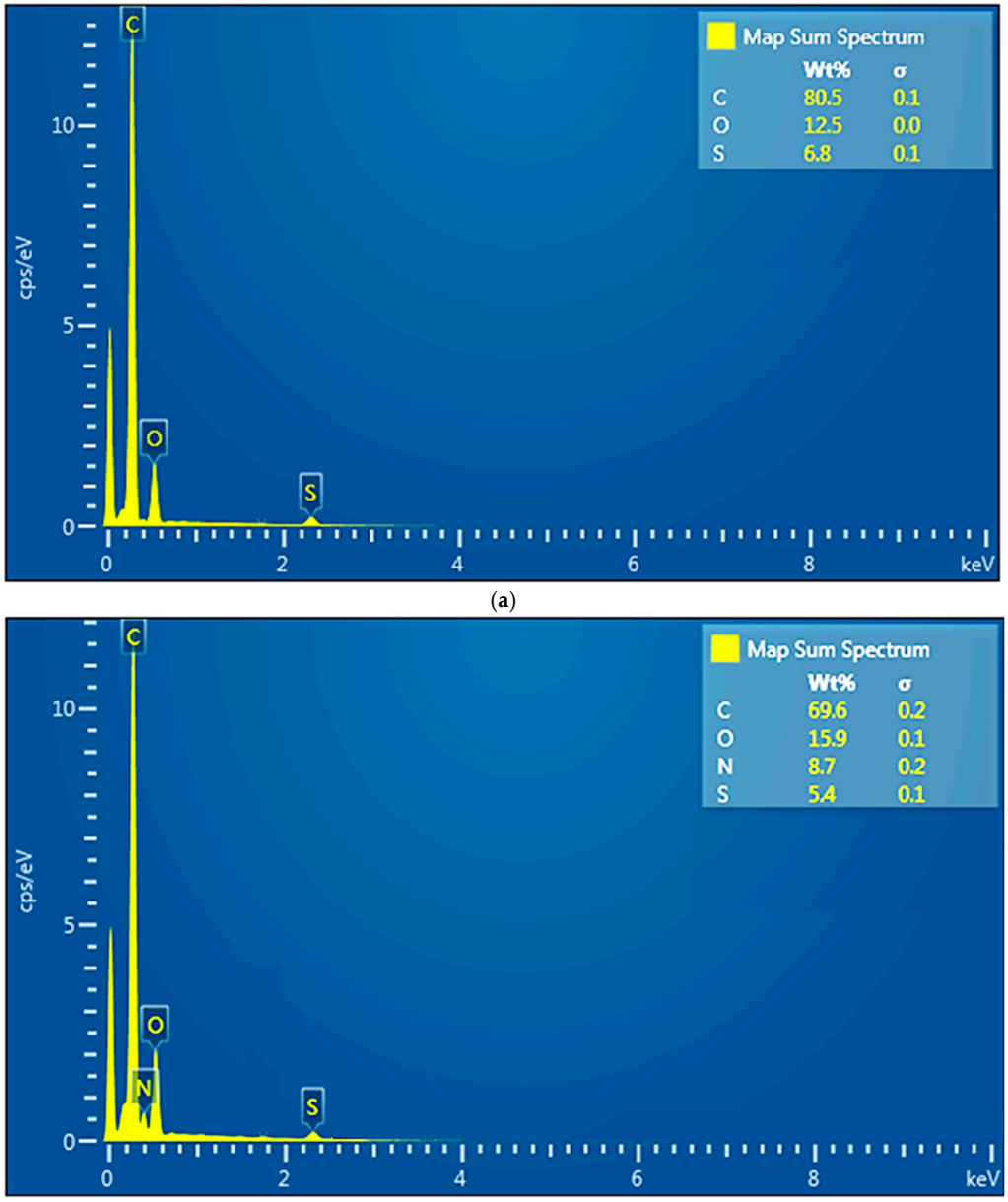


Figure 5. Energy-dispersive X-Ray spectroscopy (EDAX): (**a**) sPEEK membrane; (**b**) ABCE–sPEEK composite membrane.

The EDAX spectrum of the sPEEK membrane (Figure 5a) highlights the presence of carbon 80.5%, oxygen 12.5%, and sulfur 6.8%. The EDAX spectrum of the ABCE–sPEEK composite membrane (Figure 5b) shows the presence of carbon 69.6%, oxygen 15.5%, sulfur 5.4%, and nitrogen 8.7%. The analysis shows a decrease in the concentration of carbon and sulfur at the expense of oxygen and nitrogen. The increase in oxygen concentration is a consequence of the 4′–Amino–Benzo–15–Crown–5 Ether (ABCE) ring, and the amino group provides the nitrogen in the EDAX spectrum.

3.1.3. Thermal Analysis

Thermal analysis was performed to indicate the thermal behavior of the membranes from a scientific point of view, but also from a practical point of view (when recycling the membrane polymer through heat treatment).

The sample of the sPEEK membrane (Figure 6) presents a smaller mass loss than sPEEK in the interval RT−300 °C, only 3.12%, with the process being accompanied by a small endothermic peak at 79.8 °C and a small exothermic peak at 264.5 °C. These effects correspond with the elimination of residual solvent molecules and the beginning of the desulfurization processes. Above 300 °C, oxidative degradation becomes evident due to mass loss and associated exothermic effects, indicating the complexity of the sample and degradation reactions. The recorded mass loss between 300–475 °C is 86.41%. As indicated in Figure S1, the residual carbonaceous mass is burned after 475 °C, when a mass loss of 9.98% is recorded and the FTIR of evolved gases identifies CO_2 as the major product. Similar behavior is reported in the literature [59].

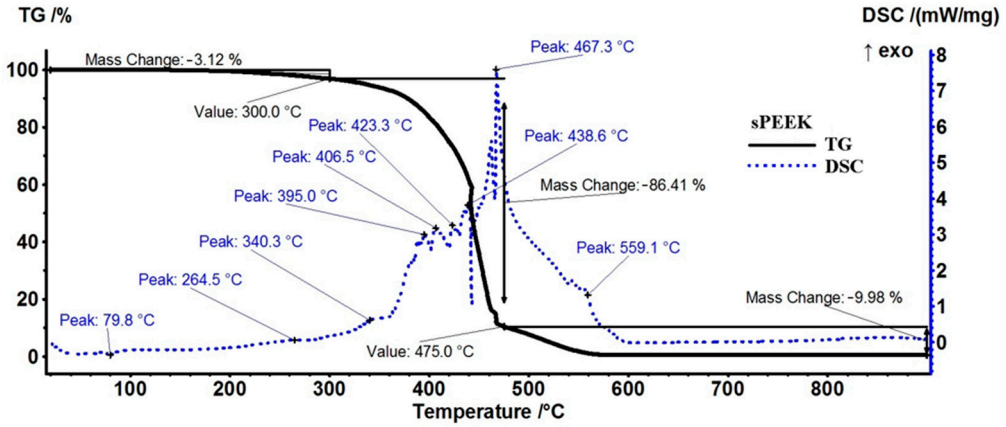


Figure 6. Diagram of thermal analysis (TG and DSC) of the sPEEK membrane.

The sample of the composite membrane (ABCE–sPEEK) (Figure 7) is stable, losing only 0.36% up to 190 °C (residual molecules of water as indicated by FTIR and by the very weak endothermic effect from 79.9 °C). Further, the sample loses 3.75% of its mass up to 300 °C, and the process is accompanied by a weak exothermic peak at 260.8 °C, indicating oxidation.

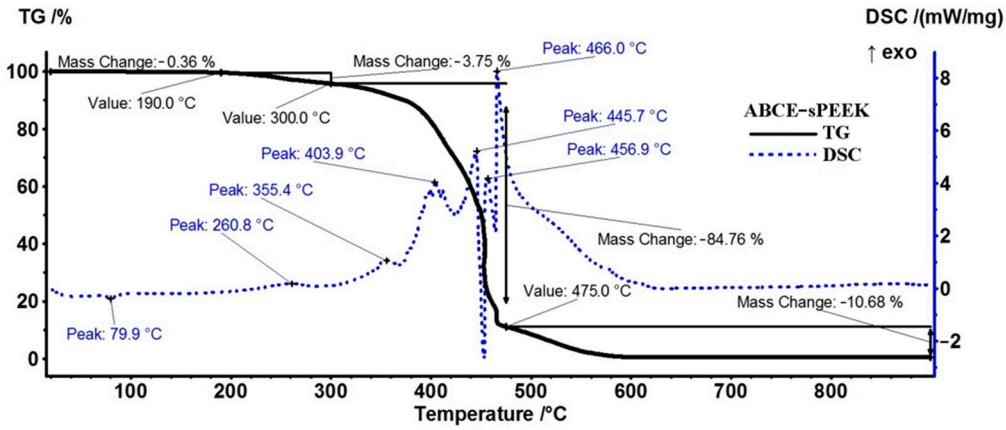


Figure 7. Diagram of thermal analysis (TG and DSC) of the ABCE–sPEEK membrane.

Between 300–475 °C, the sample loses 84.76% of its mass in a series of oxidative–degradative processes, accompanied by exothermic peaks at 355.4, 403.9, 445.7, 456.9, and 466.0 °C. The strong and quick oxidation process towards the end of the interval starts for ABCE–sPEEK at 440 °C, ~10 °C earlier than the sPEEK sample, and the exothermic peak

is placed at approximately the same temperature, 466 °C vs. 467.3 °C. The oxidation of the sample becomes highly exothermic and quick after 450 °C. After 475 °C, a mass loss of 10.68% is recorded as the residual carbonaceous mass is burned away.

3.2. The Process Performance of the Prepared Membranes

When dissolving thorium nitrate in water, hydroxyl species are formed [41,45,60,61] as shown hypothetically in Figure 8 [41,45].

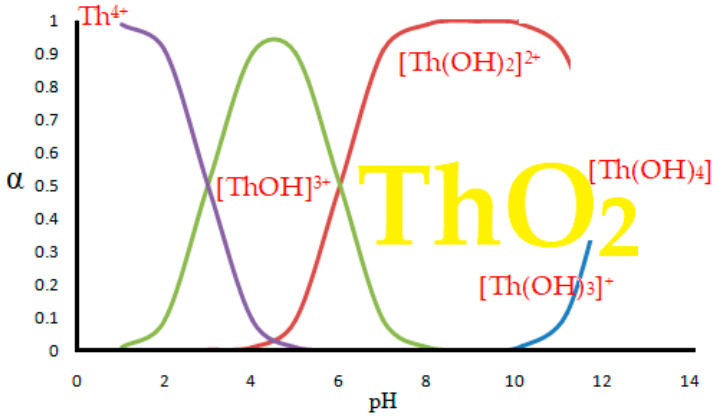


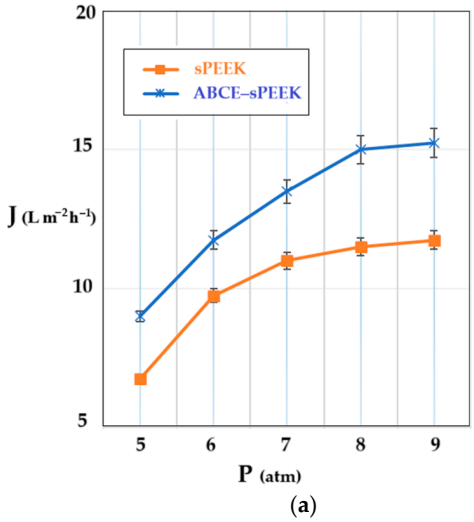
Figure 8. Hypothetical stability diagram of thorium hydroxyl complexes in aqueous media, reprinted from [41].

The degree of formation in the solution of various chemical species can be determined exactly if the acidity constants of the chemical species and/or the stability constants of the hydroxyl complexes are known [62]. The existence of chemical species of thorium can be found in Pourbaix diagrams, which take into account both the pH and the electrochemical potential of the aqueous system [63].

The appearance of thorium dioxide is also related to the pH of the solution [61,62], but in this paper we consider the separation of thorium from acidic solutions, of a pH from 0 to 4, when the predominant chemical species is Th^{4+}.

3.2.1. Determination of Hydrodynamic Performance

The determination of the hydrodynamic performance of the membranes was carried out using ultrapure water. The variable parameters were the working pressure (Figure 9a) and the rotational speed of the propeller agitator [64] (Figure 9b).



(**a**)

Figure 9. *Cont.*

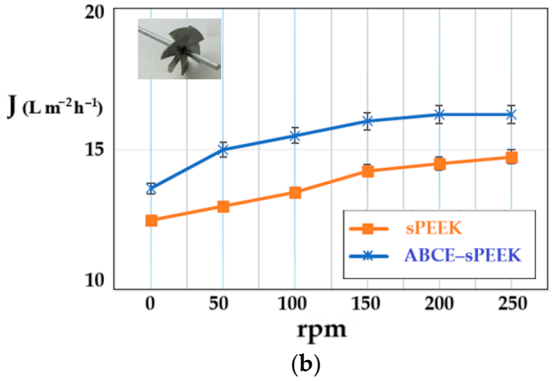


Figure 9. Dependence of permeate flux (J) on: (**a**) working pressure; (**b**) stirring regime (rpm).

The shape of the flux curves (J) as a function of the working pressure, corresponding to the sPEEK membrane and the ABCE–sPEEK composite membrane, is the same. From the obtained results, at a stirring speed of 50 rpm (Figure 9a), it appears that the working pressure causes an increase in the permeate flux (pure water), in the range of 5–8 atmospheres, after which a plateau is observed. For both membranes, the optimal working pressure is 8 atmospheres. The appearance of the flux plateau (pregnant for the sPEEK membrane) can be explained by the compaction of the membranes at high pressure. The ABCE–sPEEK membrane has a higher flux than the sPEEK membrane over the entire pressure range studied. This observation is in agreement with the porous structures on the section of two membranes presented in Figures 3a and 4a. Also, the pores on the bottom surfaces shown in Figure 3b,c for the sPEEK membrane, compared to the pores of the ABCE–sPEEK composite membrane in Figure 4b,c, justify the higher fluxes of the composite membrane.

When the pressure increased above the value of 9 atmospheres, the break-up of the membranes was observed.

On the other hand, increasing the rotation speed while operating at a pressure of 8 atmospheres (Figure 9b) causes an increase in the permeate fluxes between 50 rpm and 200 rpm, after which a plateau is observed for both membranes. The appearance of the plateau is determined by the turbulent flow regime that appears at 200 rpm and continues at the following rotation values of the propeller. The speed chosen for the subsequent studies was 200 rpm. The flow regime led to an additional flow contribution of about 20% for the sPEEK membrane and about 15% for the ABCE–sPEEK composite membrane.

The permeate fluxes, both depending on the working pressure and the rotational speed of the agitator, are higher for the ABCE–sPEEK composite membrane compared to the sPEEK membrane.

3.2.2. The Retention over the pH and the Concentration of the Thorium Ion Solution

At a working pressure of 8 atmospheres and an agitator rotation speed of 200 rpm, the retention variation according to pH was followed for the two membranes, at concentrations of 10^{-4} mol/L and 10^{-5} mol/L thorium nitrate in ultrapure water (Figure 10).

In all cases studied, the retention increases with the increase in pH. In the case of the sPEEK membrane, the retention is between 85% and 90% with a uniform increase over the entire pH range. The retention values for the sPEEK membrane are higher for the 10^{-5} mol/L concentration solution compared to the 10^{-4} mol/L concentration solution.

The thorium retention for the ABCE–sPEEK composite membrane varies between 90% and 98%, being higher for the 10^{-5} mol/L concentration solution than for the 10^{-4} mol/L concentration solution, over the entire pH range. In the case of the ABCE–sPEEK composite membrane, for both thorium concentrations studied, a jump in retention was found at pH 2. This observation is correlated with the acidity constant of sPEEK, which is between 2.0 and 2.2 (Table 2), but also with the presence of the crown ether in the form of the ammonium ion. A plausible explanation would be that the acidic, molecular form of sPEEK (R–SO_3H) passes into the basic, anionic form (R–SO_3^-) that interacts more strongly with the thorium

ion. At the same time, the crown ether specifically complexes the thorium ion, causing an increase in the retention of the ABCE–sPEEK composite membrane compared to the sPEEK membrane.

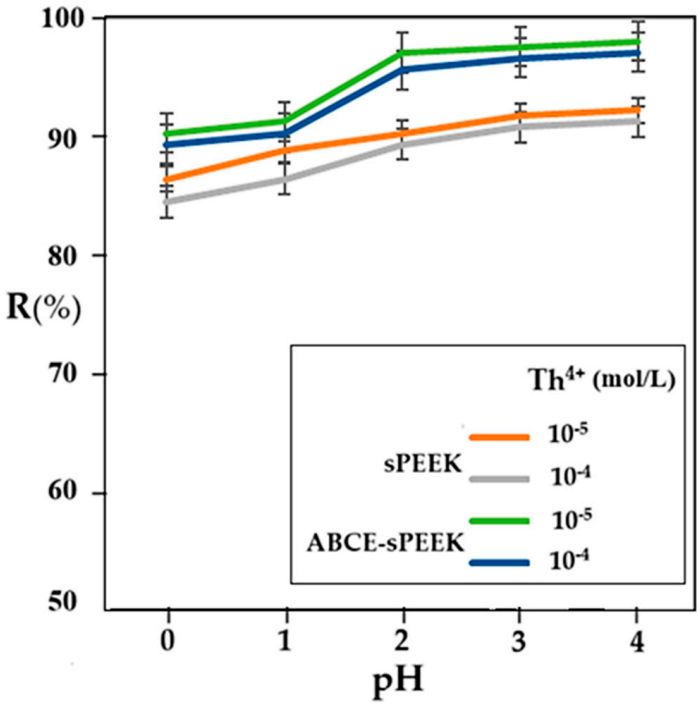


Figure 10. Dependence of retention (R%) for sPEEK membrane (orange and gray curves) and ABCE–sPEEK composite membrane (green and blue curves) for Th^{4+} solution concentration of 10^{-4} and 10^{-5} mol/L.

The previous considerations justify the superior retention of the ABCE–sPEEK composite membrane compared to the sPEEK membrane. Theoretically, for the ABCE–sPEEK composite membrane, which is more porous (Figure 4a) and has a higher flow than the less porous sPEEK membrane (Figure 3a), it would have been expected to present a lower retention.

3.2.3. Determination of Membrane Retention and Flux over Time

In order to follow the variation in the retention of the membranes depending on the operating time, the pH of the solution at the value of 4, the concentration of thorium ions of 10^{-5} mol/L, and the stirring regime of 200 rpm were chosen as parameters. Both membranes show a slight decrease in retention (Figure 11), which can be estimated to be within the acceptable limit for the dead-end nanofiltration-type working system. The retention of the ABCE–sPEEK composite membrane decreases from 98% at the first hour of operation to 95% at eight hours. For the sPEEK membrane, the decrease is from 90% in the first hour of operation to 85% after eight hours. The obtained values show that in the first hour of operation, the retention mechanism is of the adsorption type, after which it switches to the ionic expulsion regime, which determines the acceptable decrease at a relatively long operating time.

Depending on the operating regime, the evolution of the permeate flux for the thorium nitrate solution of concentration 10^{-5} mol/L and pH 4, and with the stirring regime at 200 rpm, has the same pattern for both prepared membranes (Figure 12). From the initial flux, an important decrease is observed until the fourth hour of operation, after which the flux maintains a quasi-constant value.

The performance of the ABCE–sPEEK composite membrane is superior to the performance of the sPEEK reference membrane, in all operating situations.

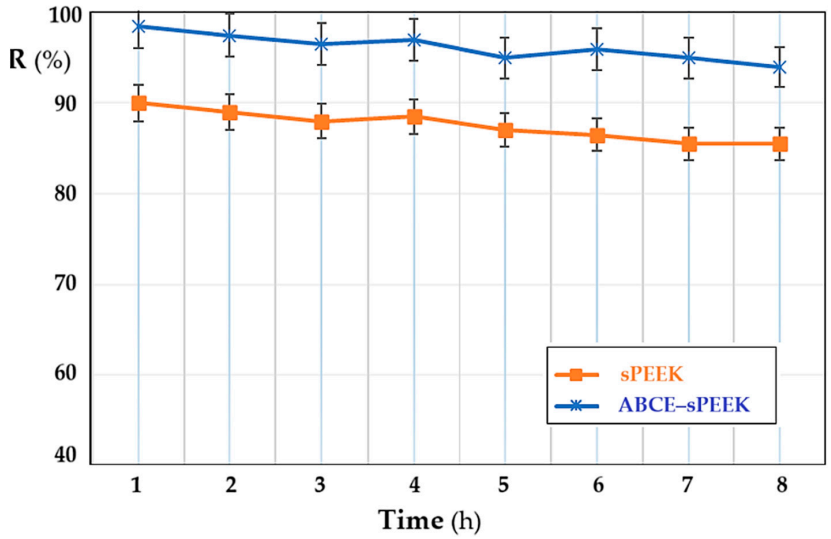


Figure 11. Dependence of retention (R%) on operating time: sPEEK membrane (in orange) and ABCE–sPEEK composite membrane (in blue).

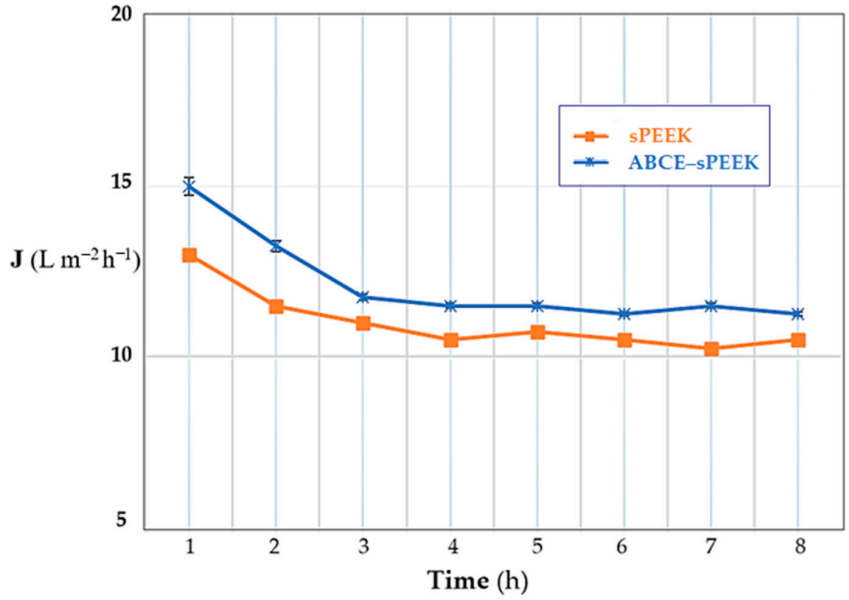


Figure 12. Dependence of the flux (J) on operating time: sPEEK membrane (in orange) and ABCE–sPEEK composite membrane (in blue).

3.2.4. The Proposed Mechanism of Thorium Ion Retention

The results obtained in this study show that the sPEEK and ABCE–sPEEK membranes retain the thorium ion through specific superficial interactions followed by ionic expulsion (Figure 13).

At a working pH, chosen between 0 and 4 units, the ionizing–complexing chemical species interact differently with the Th^{4+} ion (Table 4).

The choice of sPEEK membrane was made for comparison with the newly prepared composite membrane ABCE–sPEEK (Figure 13). The reference sPEEK membrane retains the thorium ion due to its strong acidity (pKa = 2) that manifests as such in the acidic environment) with pH 0 to pH 2, and as sulfonated anion at pH 2 to 4. The thorium ion retention occurs at the surface of the sPEEK membrane (Figure 13a,c,e). This retention of the thorium ion does not completely annihilate the 4+ charge. A large part of the thorium ion accumulates on the surface, which is justified by the ionic expulsion from the nanofiltration process [65–73].

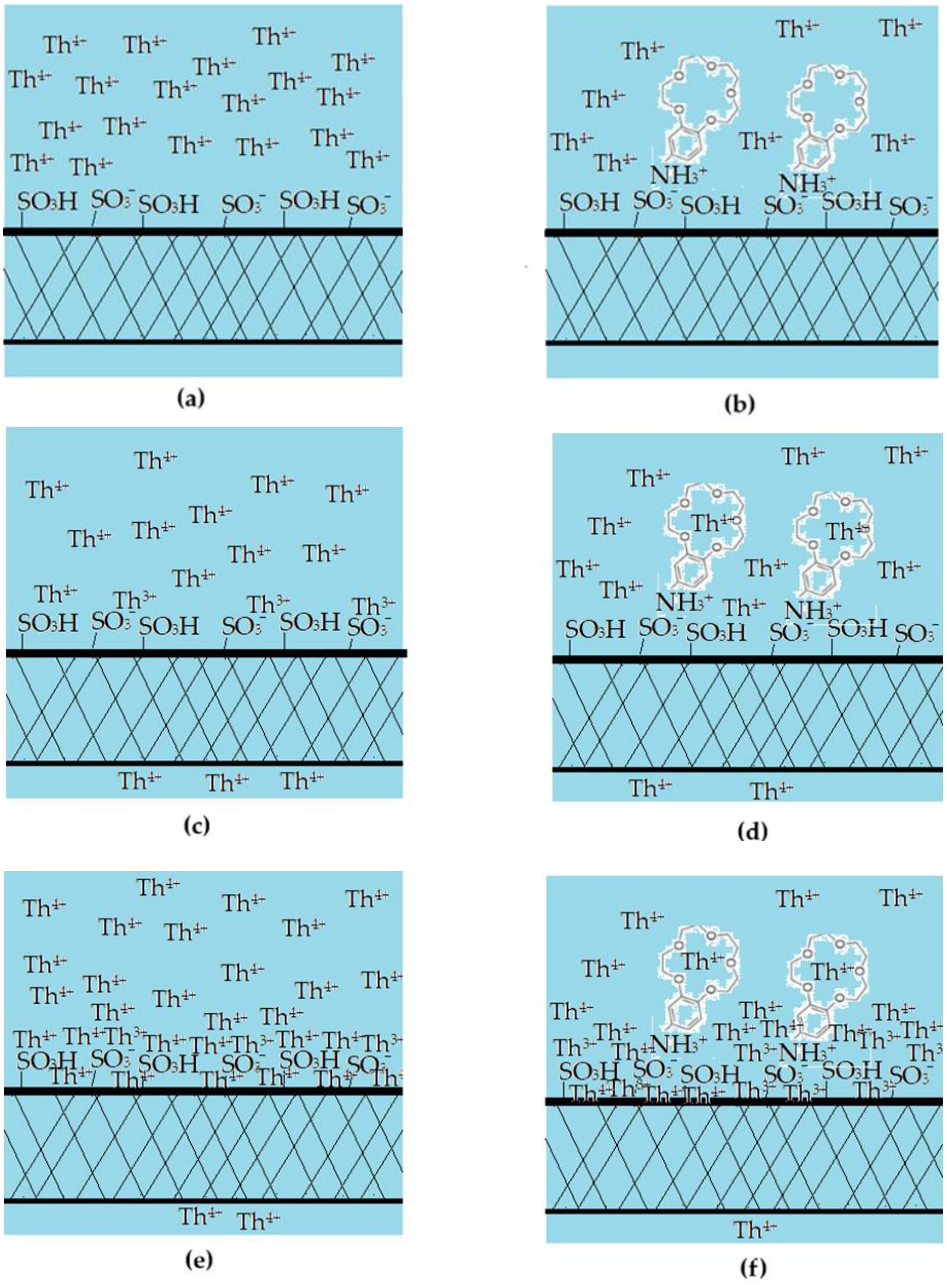


Figure 13. Schematic presentation of the proposed mechanism of thorium ion retention on sPEEK (**a**,**c**,**e**) and ABCE–sPEEK (**b**,**d**,**f**) membranes: (**a**,**b**) before nanofiltration; (**c**,**d**) beginning of nanofiltration; and (**e**,**f**) ionic expulsion nanofiltration.

Table 4. The ionizing–complexing groups of the prepared membranes depending on the pH of the aqueous solution.

Membrane		pH (Solution of Th^{4+})				
		0	**1**	**2**	**3**	**4**
The ionizing–complexing groups (Table 2)	sPEEK	R1-SO_3H	R1-SO_3H	R1-SO_3^-	R1-SO_3^-	R1-SO_3^-
	ABCE–sPEEK	R1-SO_3H R2-NH_3^+	R1-SO_3H R2-NH_3^+	R1-SO_3^- R2-NH_3^+	R1-SO_3^- R2-NH_3^+	R1-SO_3^- R2-NH_2

R1: PEEK; R2: Benzo–15C5–Ether.

In the case of the ABCE–sPEEK composite membrane (Figure 13b,d,f), it was desired to combine the effect of the sulfonic groups of sPEEK with that of ABCE. The choice of the

crown ether is justified because the ionic radius of the thorium ion (r = 179 pm) is similar to that of sodium (r = 180 pm) with which this ether specifically complexes (Figure 13b).

4. Conclusions

The toxicity of thorium is only partly related to the fact that it is a radioactive element, because its half-life is extremely long. However, being a heavy element, its removal from aqueous systems is imperative.

If we consider that it is desired to remove thorium from waters in isolated areas (for example, mining operations, mountain areas, etc.), one of the more accessible and efficient processes of doing so would be the membrane process. In this paper, nanofiltration is approached as a procedure for removing thorium from diluted synthetic aqueous solutions.

The composite membrane that is proposed in this study is made of sulfonated polyether ether ketone (sPEEK) in which Amino–Benzo–15C5–Ether (ABCE) is incorporated.

The performance of the nanofiltration process is compared between a sPEEK membrane and the composite membrane (ABCE–sPEEK), prepared by the same procedure.

The membranes were characterized by scanning electron microscopy (SEM), energy-dispersive X–Ray spectroscopy (EDAX), thermal analysis (TG and DSC), and from the perspective of thorium removal performance.

For all test parameters: pH and thorium ion concentration; working pressure; and stirring regime, the composite membrane (ABCE–sPEEK) has superior performance compared to the sPEEK membrane.

Thorium retention for the composite membrane (ABCE–sPEEK) reaches a maximum of 98% compared to the sPEEK membrane which does not exceed 90%.

The fluxes determined under the optimal conditions resulting from the study (pressure, stirring regime, concentration, and pH of the thorium solution) are a maximum of 16 $L \cdot m^{-2} \cdot h^{-1}$ for the ABCE–sPEEK composite membrane, and 15 $L \cdot m^{-2} \cdot h^{-1}$ for the sPEEK membrane.

The results obtained during the nanofiltration of the solution containing thorium are in agreement with the initially expected requirements when working with the ABCE–sPEEK membrane: selectivity/retention over 90%, operation over the entire pH range (also covering the acidic environment), maximum working pressure of 9 atmospheres, the possibility of application in isolated places, no need to use reagents or auxiliary materials, the possibility of being scaled up by simply increasing the membrane surface, and a reduction in investments.

Supplementary Materials: The following supporting information can be downloaded at: https://www.mdpi.com/article/10.3390/app14219937/s1, Figure S1. Fourier Transform Infra-Red (FTIR) spectrum at 500 °C.

Author Contributions: Conceptualization, G.N., A.C.N. and V.-A.G.; methodology, A.C.N., G.N., P.C.A. and L.M.; validation, L.M., S.-K.T. and A.R.G.; formal analysis, G.N., A.C.N., A.R.G. and L.M.; investigation, G.N., L.M., P.C.A., G.T.M., V.-A.G., A.C.N., A.R.G. and V.E.M.; resources, A.C.N., S.-K.T. and G.N.; data curation, L.M., A.C.N., A.R.G. and V.-A.G.; writing—original draft preparation, A.C.N., G.N. and V.-A.G.; writing—review and editing, G.N., A.C.N., A.R.G. and V.-A.G. All authors have read and agreed to the published version of the manuscript.

Funding: This research received no external funding.

Institutional Review Board Statement: Not applicable.

Informed Consent Statement: Not applicable.

Data Availability Statement: The original contributions presented in the study are included in the article/Supplementary Material. Further inquiries can be directed to the corresponding authors.

Acknowledgments: The authors are grateful to the Romanian Government for providing access to the research infrastructure of the National Center for Micro and Nanomaterials through the National Program titled "Installations and Strategic Objectives of National Interest". The authors gratefully acknowledge the valuable help and friendly assistance of Eng. Roxana Truşcă for performing the microscopy analysis.

Conflicts of Interest: The authors declare no conflicts of interest.

References

1. Poliakovska, K.; Annesley, I.R.; Hajnal, Z. Geophysical Constraints to the Geological Evolution and Genesis of Rare Earth Element–Thorium–Uranium Mineralization in Pegmatites at Alces Lake, SK, Canada. *Minerals* **2024**, *14*, 25. [CrossRef]
2. Jyothi, R.K.; De Melo, L.G.T.C.; Santos, R.M.; Yoon, H.S. An overview of thorium as a prospective natural resource for future energy. *Front. Energy Res.* **2023**, *11*, 1132611. [CrossRef]
3. Ushakov, S.V.; Hong, Q.-J.; Gilbert, D.A.; Navrotsky, A.; Walle, A.v.d. Thorium and Rare Earth Monoxides and Related Phases. *Materials* **2023**, *16*, 1350. [CrossRef]
4. Serge, A.B.M.; Didier, T.S.S.; Samuel, B.G.; Kranrod, C.; Omori, Y.; Hosoda, M.; Saïdou; Tokonami, S. Assessment of Radiological Risks due to Indoor Radon, Thoron and Progeny, and Soil Gas Radon in Thorium-Bearing Areas of the Centre and South Regions of Cameroon. *Atmosphere* **2023**, *14*, 1708. [CrossRef]
5. Caridi, F.; Paladini, G.; Marguccio, S.; Belvedere, A.; D'Agostino, M.; Messina, M.; Crupi, V.; Venuti, V.; Majolino, D. Evaluation of Radioactivity and Heavy Metals Content in a Basalt Aggregate for Concrete from Sicily, Southern Italy: A Case Study. *Appl. Sci.* **2023**, *13*, 4804. [CrossRef]
6. Pelić, M.; Mihaljev, Ž.; Živkov Baloš, M.; Popov, N.; Gavrilović, A.; Jug-Dujaković, J.; Ljubojević Pelić, D. The Activity of Natural Radionuclides Th-232, Ra-226, K-40, and Na-22, and Anthropogenic Cs-137, in the Water, Sediment, and Common Carp Produced in Purified Wastewater from a Slaughterhouse. *Sustainability* **2023**, *15*, 12352. [CrossRef]
7. Gilbert, B.; Carrero, S.; Dong, W.; Joe-Wong, C.; Arora, B.; Fox, P.; Nico, P.; Williams, K.H. River thorium concentrations can record bedrock fracture processes including some triggered by distant seismic events. *Nat. Commun.* **2023**, *14*, 2395. [CrossRef] [PubMed]
8. Patel, K.S.; Sharma, S.; Maity, J.P.; Martín-Ramos, P.; Fiket, Ž.; Bhattacharya, P.; Zhu, Y. Occurrence of uranium, thorium and rare earth elements in the environment: A review. *Front. Environ. Sci.* **2023**, *10*, 1058053. [CrossRef]
9. Manchanda, V.K. Thorium as an abundant source of nuclear energy and challenges in separation science. *Radiochim. Acta* **2023**, *111*, 243–263. [CrossRef]
10. Aita, S.K.; Abdel-Azeem, M.M.; Abu Khoziem, H.A.; Aly, G.A.; Mahdy, N.M.; Ismail, A.M.; Ali, H.H. Tracking of uranium and thorium natural distribution in the chemical fractions of the Nile Valley and the Red Sea phosphorites, Egypt. *Carbonates Evaporites* **2024**, *39*, 32. [CrossRef]
11. Fesenko, S.V.; Emlyutina, E.S. Thorium Concentrations in Terrestrial and Freshwater Organisms: A Review of the World Data. *Biol. Bull.* **2023**, *50*, 3330–3341. [CrossRef]
12. Soesoo, A.; Vind, J.; Hade, S. Uranium and Thorium Resources of Estonia. *Minerals* **2020**, *10*, 798. [CrossRef]
13. Fesenko, S.V.; Emlutina, E.S. Thorium concentrations in the environment: A review of the global data. *Biol. Bull.* **2021**, *48*, 2086–2097. [CrossRef]
14. Humphrey, U.E.; Khandaker, M.U. Viability of thorium-based nuclear fuel cycle for the next generation nuclear reactor: Issues and prospects. *Renew. Sustain. Energy Rev.* **2018**, *97*, 259–275. [CrossRef]
15. Guo, G.L.; Lu, Y.; Yang, D.D.; Li, X.H.; Gong, M.M. Purification of thorium by precipitation. *J. Radioanal. Nucl. Chem.* **2021**, *327*, 667–671. [CrossRef]
16. Salehuddin, A.H.J.M.; Ismail, A.F.; Aziman, E.S.; Mohamed, N.A.; Teridi, M.A.M.; Idris, W.M.R. Production of high-purity ThO_2 from monazite ores for thorium fuel-based reactor. *Prog. Nucl. Energy* **2021**, *136*, 103728. [CrossRef]
17. Arabi, H.R.; Milani, S.A.; Abolghasemi, H.; Zahakifar, F. Recovery and transport of thorium (IV) through polymer inclusion membrane with D2EHPA from nitric acid solutions. *J. Radioanal. Nucl. Chem.* **2021**, *327*, 653–665. [CrossRef]
18. Lu, J.; He, K.; Wang, Y.; Chen, G.; Weng, H.; Lin, M. An Effective Process for the Separation of U(VI), Th(IV) from Rare Earth Elements by Using Ionic Liquid Cyphos IL 104. *Chin. Chem. Lett.* **2022**, *33*, 3422–3428. [CrossRef]
19. Kukkonen, E.; Virtanen, E.J.; Moilanen, J.O. α-Aminophosphonates, -Phosphinates, and -Phosphine Oxides as Extraction and Precipitation Agents for Rare Earth Metals, Thorium, and Uranium: A Review. *Molecules* **2022**, *27*, 3465. [CrossRef]
20. Zhang, H.; Gao, Y. Polymeric Materials for Rare Earth Elements Recovery. *Gels* **2023**, *9*, 775. [CrossRef]
21. Saleh, T.A.; Sarı, A.; Tuzen, M. Development and characterization of bentonite-gum arabic composite as novel highly-efficient adsorbent to remove thorium ions from aqueous media. *Cellulose* **2021**, *28*, 10321–10333. [CrossRef]
22. Safiulina, A.M.; Lizunov, A.V.; Semenov, A.A.; Baulin, D.V.; Baulin, V.E.; Tsivadze, A.Y.; Aksenov, S.M.; Tananaev, I.G. Recovery of Uranium, Thorium, and Other Rare Metals from Eudialyte Concentrate by a Binary Extractant Based on 1,5-bis[2-(hydroxyethoxyphosphoryl)-4-ethylphenoxy]-3-oxapentane and Methyl Trioctylammonium Nitrate. *Minerals* **2022**, *12*, 1469. [CrossRef]
23. Aydin, F.A.; Soylak, M. Separation, preconcentration and inductively coupled plasma-mass spectrometric (ICP-MS) determination of thorium(IV), titanium(IV), iron(III), lead(II) and chromium(III) on 2-nitroso-1-naphthol impregnated MCI GEL CHP20P resin. *J. Hazard. Mater.* **2010**, *173*, 669–674. [CrossRef] [PubMed]
24. Moghaddam, Z.S.; Kaykhaii, M.; Khajeh, M.; Oveisi, A.R. Synthesis of UiO-66-OH zirconium metal-organic framework and its application for selective extraction and trace determination of thorium in water samples by spectrophotometry. *Spectrochim. Acta Part A Mol. Biomol. Spectrosc.* **2018**, *194*, 76–82. [CrossRef] [PubMed]
25. Georgiou, E.; Pashalidis, I.; Raptopoulos, G.; Paraskevopoulou, P. Efficient Removal of Polyvalent Metal Ions (Eu(III) and Th(IV)) from Aqueous Solutions by Polyurea-Crosslinked Alginate Aerogels. *Gels* **2022**, *8*, 478. [CrossRef]

26. Kuang, S.; Zhang, Z.; Li, Y.; Wu, G.; Wei, H.; Liao, W. Selective Extraction and Separation of Ce(IV) from Thorium and Trivalent Rare Earths in Sulfate Medium by an α-Aminophosphonate Extractant. *Hydrometallurgy* **2017**, *167*, 107–114. [CrossRef]
27. Salah, B.A.; Gaber, M.S.; Kandil, A.H.T. The Removal of Uranium and Thorium from Their Aqueous Solutions by 8-Hydroxyquinoline Immobilized Bentonite. *Minerals* **2019**, *9*, 626. [CrossRef]
28. Felix, C.S.A.; Chagas, A.V.B.; de Jesus, R.F.; Barbosa, W.T.; Barbosa, J.D.V.; Ferreira, S.L.C.; Cerdà, V. Synthesis and Application of a New Polymer with Imprinted Ions for the Preconcentration of Uranium in Natural Water Samples and Determination by Digital Imaging. *Molecules* **2023**, *28*, 4065. [CrossRef]
29. Talan, D.; Huang, Q. Separation of Radionuclides from a Rare Earth-Containing Solution by Zeolite Adsorption. *Minerals* **2021**, *11*, 20. [CrossRef]
30. Sabbatovskii, K.G. The effect of the adsorption of multicharge cations on the selectivity of a nanofiltration membrane. *Colloid J.* **2003**, *65*, 237–243. [CrossRef]
31. Gonçalves, A.R.P.; Paredes, X.; Cristino, A.F.; Santos, F.J.V.; Queirós, C.S.G.P. Ionic Liquids—A Review of Their Toxicity to Living Organisms. *Int. J. Mol. Sci.* **2021**, *22*, 5612. [CrossRef] [PubMed]
32. Rybak, A.; Rybak, A.; Kolev, S.D. A Modern Computer Application to Model Rare Earth Element Ion Behavior in Adsorptive Membranes and Materials. *Membranes* **2023**, *13*, 175. [CrossRef] [PubMed]
33. Kaptakov, V.O.; Milyutin, V.V.; Nekrasova, N.A.; Zelenin, P.G.; Kozlitin, E.A. Nanofiltration Extraction of Uranium and Thorium from Aqueous Solutions. *Radiochemistry* **2021**, *63*, 169–172. [CrossRef]
34. Ardehali, B.A.; Zaheri, P.; Yousefi, T. The effect of operational conditions on the stability and efficiency of an emulsion liquid membrane system for removal of uranium. *Prog. Nucl. Energy* **2020**, *130*, 103532. [CrossRef]
35. Laguel, S.; Samar, M.H. Elimination of rare earth (neodymium (III)) from water by emulsion liquid membrane process using D2EHPA as a carrier in kerosene. *Desalination Water Treat.* **2024**, *317*, 100214. [CrossRef]
36. Allahyari, S.A.; Minuchehr, A.; Ahmadi, S.J.; Charkhi, A. Thorium pertraction through hollow fiber renewal liquid membrane (HFRLM) using Cyanex 272 as carrier. *Prog. Nucl. Energy* **2017**, *100*, 209–220. [CrossRef]
37. Ammari Allahyari, S.; Charkhi, A.; Ahmadi, S.J.; Minuchehr, A. Modeling and experimental validation of the steady-state counteractive facilitated transport of Th (IV) and hydrogen ions through hollow-fiber renewal liquid membrane. *Chem. Pap.* **2021**, *75*, 325–336. [CrossRef]
38. Milani, S.A.; Zahakifar, F.; Faryadi, M. Membrane assisted transport of thorium (IV) across bulk liquid membrane containing DEHPA as ion carrier: Kinetic, mechanism and thermodynamic studies. *Radiochim. Acta* **2022**, *110*, 841–852. [CrossRef]
39. Lankapati, H.M.; Dankhara, P.M.; Lathiya, D.R.; Shah, B.; Chudasama, U.V.; Choudhary, L.; Maheria, K.C. Removal of lanthanum, cerium and thorium metal ions from aqueous solution using ZrT hybrid ion exchanger. *Sustain. Energy Technol. Assess.* **2021**, *47*, 101415. [CrossRef]
40. Aziman, E.S.; Mohd Salehuddin, A.H.J.; Ismail, A.F. Remediation of thorium (IV) from wastewater: Current status and way forward. *Sep. Purif. Rev.* **2021**, *50*, 177–202. [CrossRef]
41. Man, G.T.; Albu, P.C.; Nechifor, A.C.; Grosu, A.R.; Tanczos, S.-K.; Grosu, V.-A.; Ioan, M.-R.; Nechifor, G. Thorium Removal, Recovery and Recycling: A Membrane Challenge for Urban Mining. *Membranes* **2023**, *13*, 765. [CrossRef] [PubMed]
42. Covaliu-Mierlă, C.I.; Păunescu, O.; Iovu, H. Recent Advances in Membranes Used for Nanofiltration to Remove Heavy Metals from Wastewater: A Review. *Membranes* **2023**, *13*, 643. [CrossRef] [PubMed]
43. Mahmoud, A.E.D.; Mostafa, E. Nanofiltration Membranes for the Removal of Heavy Metals from Aqueous Solutions: Preparations and Applications. *Membranes* **2023**, *13*, 789. [CrossRef] [PubMed]
44. Moreira, J.B.; Santos, T.D.; Zaparoli, M.; de Almeida, A.C.A.; Costa, J.A.V.; de Morais, M.G. An Overview of Nanofiltration and Nanoadsorption Technologies to Emerging Pollutants Treatment. *Appl. Sci.* **2022**, *12*, 8352. [CrossRef]
45. Man, G.T.; Albu, P.C.; Nechifor, A.C.; Grosu, A.R.; Popescu, D.I.; Grosu, V.-A.; Marinescu, V.E.; Nechifor, G. Simultaneously Recovery of Thorium and Tungsten through Hybrid Electrolysis–Nanofiltration Processes. *Toxics* **2024**, *12*, 103. [CrossRef]
46. Cimbru, A.M.; Rikabi, A.A.K.K.; Oprea, O.; Grosu, A.R.; Tanczos, S.-K.; Simonescu, M.C.; Pașcu, D.; Grosu, V.-A.; Dumitru, F.; Nechifor, G. *pH* and *pCl* Operational Parameters in Some Metallic Ions Separation with Composite Chitosan/Sulfonated Polyether Ether Ketone/Polypropylene Hollow Fibers Membranes. *Membranes* **2022**, *12*, 833. [CrossRef]
47. Nechifor, A.C.; Ruse, E.; Nechifor, G.; Serban, B. Membrane materials. II. Electrodialysis with membranes of chemically modified polyetherketones. *Rev. Chim.* **2002**, *53*, 472–482.
48. Baicea, C.; Nechifor, A.C.; Vaireanu, D.I.; Gales, O.; Trusca, R.; Voicu, S.I. Sulfonated poly (ether ether ketone)–activated polypyrrole composite membranes for fuel cells. *Optoelectron. Adv. Mater.-Rapid Commun.* **2011**, *5*, 1181–1185.
49. Din, I.S.; Cimbru, A.M.; Rikabi, A.A.K.K.; Tanczos, S.K.; Ticu Cotorcea, S.; Nechifor, G. Iono-molecular Separation with Composite Membranes VI. Nitro-phenol separation through sulfonated polyether ether ketone on capillary polypropylene membranes. *Rev. Chim.* **2018**, *69*, 1603–1607. [CrossRef]
50. Zhu, Y.; Galier, S.; Roux-de Balmann, H. Description of the variation of retention versus pH in nanofiltration of organic acids. *J. Membr. Sci.* **2021**, *637*, 119588. [CrossRef]
51. Nashine, N.; Deb, M.K.; Mishra, R.K. Spectrophotometric determination of thorium in standard samples and monazite sands based on the floated complex of thorium with N-hydroxy-N,N′-diphenylbenzamidine and thorin. *Anal Bioanal Chem.* **1996**, *355*, 34–36. [CrossRef] [PubMed]

52. Prioteasa, P.; Marinescu, V.; Bara, A.; Iordoc, M.; Teisanu, A.; Banciu, C.; Meltzer, V. Electrodeposition of Polypyrrole on Carbon Nanotubes/Si in the Presence of Fe Catalyst for Application in Supercapacitors. *Rev. Chim.* **2015**, *66*, 820–824.
53. Zamfir, L.-G.; Rotariu, L.; Marinescu, V.E.; Simelane, X.T.; Baker, P.G.L.; Iwuoha, E.I.; Bala, C. Non-enzymatic polyamic acid sensors for hydrogen peroxide detection. *Sens. Actuators B Chem.* **2016**, *226*, 525–533. [CrossRef]
54. Chircov, C.; Bejenaru, I.T.; Nicoară, A.I.; Bîrcă, A.C.; Oprea, O.C.; Tihăuan, B. Chitosan-Dextran-Glycerol Hydrogels Loaded with Iron Oxide Nanoparticles for Wound Dressing Applications. *Pharmaceutics* **2022**, *14*, 2620. [CrossRef]
55. Dimulescu, I.A.; Nechifor, A.C.; Bărdacă, C.; Oprea, O.; Paşcu, D.; Totu, E.E.; Albu, P.C.; Nechifor, G.; Bungău, S.G. Accessible Silver-Iron Oxide Nanoparticles as a Nanomaterial for Supported Liquid Membranes. *Nanomaterials* **2021**, *11*, 1204. [CrossRef] [PubMed]
56. Nechifor, G.; Păncescu, F.M.; Albu, P.C.; Grosu, A.R.; Oprea, O.; Tanczos, S.-K.; Bungău, C.; Grosu, V.-A.; Ioan, M.-R.; Nechifor, A.C. Transport and Separation of the Silver Ion with *n*–decanol Liquid Membranes Based on 10–undecylenic Acid, 10–undecen–1–ol and Magnetic Nanoparticles. *Membranes* **2021**, *11*, 936. [CrossRef] [PubMed]
57. Nechifor, G.; Grosu, A.R.; Ferencz, A.; Tanczos, S.-K.; Goran, A.; Grosu, V.-A.; Bungău, S.G.; Păncescu, F.M.; Albu, P.C.; Nechifor, A.C. Simultaneous Release of Silver Ions and 10–Undecenoic Acid from Silver Iron–Oxide Nanoparticles Impregnated Membranes. *Membranes* **2022**, *12*, 557. [CrossRef]
58. Nechifor, A.C.; Pîrțac, A.; Albu, P.C.; Grosu, A.R.; Dumitru, F.; Dimulescu, I.A.; Oprea, O.; Pașcu, D.; Nechifor, G.; Bungău, S.G. Recuperative Amino Acids Separation through Cellulose Derivative Membranes with Microporous Polypropylene Fiber Matrix. *Membranes* **2021**, *11*, 429. [CrossRef]
59. Motelica, L.; Ficai, D.; Petrisor, G.; Oprea, O.-C.; Trușcă, R.-D.; Ficai, A.; Andronescu, E.; Hudita, A.; Holban, A.M. Antimicrobial Hydroxyethyl-Cellulose-Based Composite Films with Zinc Oxide and Mesoporous Silica Loaded with Cinnamon Essential Oil. *Pharmaceutics* **2024**, *16*, 1225. [CrossRef]
60. Guo, P.; Duan, T.; Song, X.; Xu, J.; Chen, H. Effects of soil pH and organic matter on distribution of thorium fractions in soil contaminated by rare-earth industries. *Talanta* **2008**, *77*, 624–627. [CrossRef]
61. Langmuir, D.; Herman, J.S. The mobility of thorium in natural waters at low temperatures. *Geochim. Cosmochim. Acta* **1980**, *44*, 1753–1766. [CrossRef]
62. Wang, X.; Huang, W.; Gong, Y.; Jiang, F.; Zheng, H.; Zhu, T.; Long, D.; Li, Q. Electrochemical behavior of Th (IV) and its electrodeposition from ThF4-LiCl-KCl melt. *Electrochim. Acta* **2016**, *196*, 286–293. [CrossRef]
63. Delpech, S.; Carrière, C.; Chmakoff, A.; Martinelli, L.; Rodrigues, D.; Cannes, C. Corrosion Mitigation in Molten Salt Environments. *Materials* **2024**, *17*, 581. [CrossRef] [PubMed]
64. Pîrțac, A.; Nechifor, A.C.; Tanczos, S.-K.; Oprea, O.C.; Grosu, A.R.; Matei, C.; Grosu, V.-A.; Vasile, B.Ș.; Albu, P.C.; Nechifor, G. Emulsion Liquid Membranes Based on Os–NP/n–Decanol or n–Dodecanol Nanodispersions for p–Nitrophenol Reduction. *Molecules* **2024**, *29*, 1842. [CrossRef] [PubMed]
65. Żyłła, R.; Ledakowicz, S.; Boruta, T.; Olak-Kucharczyk, M.; Foszpańczyk, M.; Mrozińska, Z.; Balcerzak, J. Removal of Tetracycline Oxidation Products in the Nanofiltration Process. *Water* **2021**, *13*, 555. [CrossRef]
66. Suhalim, N.S.; Kasim, N.; Mahmoudi, E.; Shamsudin, I.J.; Mohammad, A.W.; Mohamed Zuki, F.; Jamari, N.L.-A. Rejection Mechanism of Ionic Solute Removal by Nanofiltration Membranes: An Overview. *Nanomaterials* **2022**, *12*, 437. [CrossRef]
67. Sewerin, T.; Elshof, M.G.; Matencio, S.; Boerrigter, M.; Yu, J.; de Grooth, J. Advances and Applications of Hollow Fiber Nanofiltration Membranes: A Review. *Membranes* **2021**, *11*, 890. [CrossRef]
68. Tapia-Quirós, P.; Montenegro-Landívar, M.F.; Reig, M.; Vecino, X.; Saurina, J.; Granados, M.; Cortina, J.L. Integration of Nanofiltration and Reverse Osmosis Technologies in Polyphenols Recovery Schemes from Winery and Olive Mill Wastes by Aqueous-Based Processing. *Membranes* **2022**, *12*, 339. [CrossRef]
69. Bóna, Á.; Galambos, I.; Nemestóthy, N. Progress towards Stable and High-Performance Polyelectrolyte Multilayer Nanofiltration Membranes for Future Wastewater Treatment Applications. *Membranes* **2023**, *13*, 368. [CrossRef]
70. Turek, M.; Mitko, K.; Skóra, P.; Dydo, P.; Jakóbik-Kolon, A.; Warzecha, A.; Tyrała, K. Improving the Performance of a Salt Production Plant by Using Nanofiltration as a Pretreatment. *Membranes* **2022**, *12*, 1191. [CrossRef]
71. Ahmad, N.N.R.; Mohammad, A.W.; Mahmoudi, E.; Ang, W.L.; Leo, C.P.; Teow, Y.H. An Overview of the Modification Strategies in Developing Antifouling Nanofiltration Membranes. *Membranes* **2022**, *12*, 1276. [CrossRef] [PubMed]
72. Jafarinejad, S.; Esfahani, M.R. A Review on the Nanofiltration Process for Treating Wastewaters from the Petroleum Industry. *Separations* **2021**, *8*, 206. [CrossRef]
73. Ali, M.E.A. Nanofiltration Process for Enhanced Treatment of RO Brine Discharge. *Membranes* **2021**, *11*, 212. [CrossRef] [PubMed]

Disclaimer/Publisher's Note: The statements, opinions and data contained in all publications are solely those of the individual author(s) and contributor(s) and not of MDPI and/or the editor(s). MDPI and/or the editor(s) disclaim responsibility for any injury to people or property resulting from any ideas, methods, instructions or products referred to in the content.